

Research
paper

Fluid hammer phenomena for Nitromethane propellant feed system

Ryojiro Minato^{*†} and Shigeru Tanaka^{**}

^{*}Department of Engineering, Muroran Institute of Technology, 27-1 Mizumoto-cho, Muroran, Hokkaido 050-8585, JAPAN
Phone: +81-143-46-5378

[†]Corresponding author: r-minato@mmm.muroran-it.ac.jp

^{**}Institute of Industrial Nanomaterials (IINa), the University of Kumamoto 2-39-1 Kurokami, Chuo-ku, Kumamoto 860-8555, JAPAN

Received: February 16, 2022 Accepted: June 15, 2022

Abstract

The present study explores the explosion risk of nitromethane in fluid hammer phenomena. Nitromethane flowed through the flowpath by the gas-pressurized feed method in this test. The tank pressure conditions are 0.4, 0.6, 0.8 and 0.95 MPaG. No explosion occurred in any case in the present study. The fluid hammer test of water is also conducted to compare with nitromethane. The experimental peak pressure is 5.15 MPaG, and the fluid hammer pressure rise is 4.59 MPaG in the tank pressure condition of 0.95 MPaG. The experimental pressure rise of nitromethane is close to the theoretical prediction given by the Joukowsky equation in the flow velocity condition of more than $3.0 \text{ m} \cdot \text{s}^{-1}$ if the pressure propagation velocity is equal to the sonic speed. The peak pressure of the fluid hammer effect for water is the same with or higher than nitromethane. The other experimental fluid hammer test data indicates that nitromethane has similar fluid dynamic behaviors to water. Thus, the present investigation recommends using water for the fluid hammer test of the nitromethane feed system.

Keywords: Nitromethane, water hammer phenomena, explosion

NOMENCLATURE

a	Speed of Sound or Pressure Propagation Speed [$\text{m} \cdot \text{s}^{-1}$]
D	Inner Diameter of Pipe
E	Elasticity [Pa]
p	Pressure [Pa]
t	Wall Thickness of Pipe
v	Flow Velocity [$\text{m} \cdot \text{s}^{-1}$]
ρ	Density [$\text{kg} \cdot \text{m}^{-3}$]

Subscript

F	Liquid Fluid
P	Pipe

1. Introduction

Nitromethane is the simplest nitro compound and has been widely used as a model substance for examining the physical and chemical properties of explosives. Nelson employed nitromethane to investigate photodissociation

mechanisms in high explosive materials¹⁾ Tanaka et al. investigated the nitromethane reaction with light metal vapor or tungsten²⁾. They reported that the oxidation of aluminum or magnesium promoted nitromethane deflagration²⁾. Moreover, Takahashi et al. investigated the reaction of nitromethane by electronic discharge in liquid phase³⁾. After World War 2, many researchers considered nitromethane as a candidate for rocket-propellant and conducted its combustion tests. However, those studies found nitromethane has ignition difficulty. On the other hand, hydrazine or its derivatives have excellent ignition ability and are suitable for space propulsion. Therefore nitromethane has been scarcely used for space propulsion⁴⁾. Unfortunately, hydrazine and its derivatives are toxic liquids and have difficulties in handling them. The demand for low toxic liquid propellant has always arisen. Therefore, nitromethane is expected again as an alternative propellant due to its low toxicity and safety^{5), 6)}. Nitromethane can burn without oxygen due to its nitro group. Thus, it is applicable as a liquid monopropellant.

Nitromethane has been used in electric discharge

fracturing technology by using its deflagration phenomenon^{7)–9)}. Nitromethane has shock resistance and is a relatively safe substance. Thus, an extreme high shock pressure is required for an initiation of detonation in nitromethane. For example, Bouyer *et al.* conducted the detonation experiment with plane shock impact of 8.6 GPa¹⁰⁾. For example, an explosive accident of nitromethane occurred in 1958 at Mount Pulaski in Illinois, USA¹¹⁾. It is speculated that a rapid shutoff of a valve in the nitromethane flowpath pipe could cause an adiabatic compression, which create a hammer-lock pressure surge¹²⁾. When the air bubble entrained in nitromethane, it turns to be adiabatically compressed by the rapid valve closing, resulting in rapid rises in temperature and pressure. This temperature rise can cause the explosion¹²⁾. ANGUS chemical company reports that the following situation should be avoided in handling nitromethane, 1) severe impact, 2) rapid pressurization in a closed space, and 3) heating in a closed space¹³⁾.

The manipulation of valves can control the liquid propellant flow in the satellite propellant feed system. Rapid closing of a valve can cause fluid hammer phenomena. Nitromethane is insensitive to an explosion. However, those fluid hammer phenomena involve a severe impact in a closed space, which should be avoided, as ANGUS chemical company report warned. The design of the satellite reaction control system (RCS) requires quantitating the explosive sensitivity of nitromethane. Thus, the authors conducted fluid hammer tests of nitromethane to evaluate its pressure impact for its application to the RCS. A severe pressure impact can cause an explosive accident for nitromethane. At the same time, the authors also did the fluid hammer tests of water in the present study to compare its fluid hammer phenomena with nitromethane. The data of the fluid hammer phenomena for water is applicable in the estimation of the pressure impact for nitromethane if any similarities exist in the fluid hammer phenomena of both fluids. The experimental results in the present study will provide the design and operational criteria for the future practical use of nitromethane-propellant for space propulsion.

2. Experimental device and methods

2.1 Characteristics of fluid hammer phenomena

The pressure rise by fluid hammer effect is usually predicted by the Joukowsky equation. Equation (1) indicates this theoretical prediction for fluid hammer phenomena.

$$\Delta p = \rho a \Delta v \quad (1)$$

Δv is the velocity variant by the valve closure. It may be equal to the flow velocity before the valve shuts off. a is the pressure propagation velocity, which is equal to the speed of sound in the liquid. The speed of sound in liquid is given by the volumetric elasticity, E_F , and liquid density, ρ .

$$a = \sqrt{\frac{E_F}{\rho}} \quad (2)$$

In fluid hammer phenomena, the pressure propagation velocity is given by Allievi's equation. Allievi's theory includes the elasticity of the pipe material in consideration.

$$a = \frac{1}{\sqrt{\rho \left(\frac{1}{E_F} + \frac{1}{E_P} \frac{D}{t} \right)}} \quad (3)$$

The pressure propagation velocity is estimated by Equation (2) if the effect of E_P is negligible, such as the underground pipes. The liquid temperature usually affects the speeds of sound. The water temperature was 297.3 ± 0.8 K during the present tests, and the nitromethane temperature was 294.2 ± 1.5 K. From those temperature data, the speed of sound is evaluated as $1494.6 \text{ m} \cdot \text{s}^{-1}$ in water by using the table presented by Greenspan and Tschiegg¹⁴⁾. The speed of sound in nitromethane is estimated as $1335.9 \text{ m} \cdot \text{s}^{-1}$ by using the data of Cwiklinska and Kinart¹⁵⁾. Thus, the volumetric elasticities of water and nitromethane are calculated as 2.234 GPa and 2.031 GPa, respectively. The theoretical fluid hammer pressure rises are based on those speeds of sound data in the present study.

2.2 Experimental apparatus and facility

The authors conducted the fluid hammer test to investigate the explosion risk of nitromethane. Because of the explosion risk, the authors employ the explosion chamber in the institute of industrial nanomaterials, the University of Kumamoto, in the present study. Figures 1 and 2 show the photo of the experimental apparatus and its detailed layout, respectively. The feed flowpath pipe comes out from the bottom of the nitromethane tank, and two solenoid valves are arranged in series on the way of this flowpath pipe. Figure 3 shows the system diagram of this experimental device.

The simultaneous closing of the two solenoid valves let the fluid hammer phenomena occur during the flow test. The flowpath pipe between those two valves forms the confinement section, and this confinement section can make a rapid pressure rise of the fluid hammer phenomenon as high as possible. Those two solenoid valves are AB41E4 by CKD Corporation[®] and the explosion-proof type. The authors use two pressure transducers of PGS-100KA by Kyowa Electronic Instruments[®] to measure the fluid pressure upstream of each two valves. In addition, the

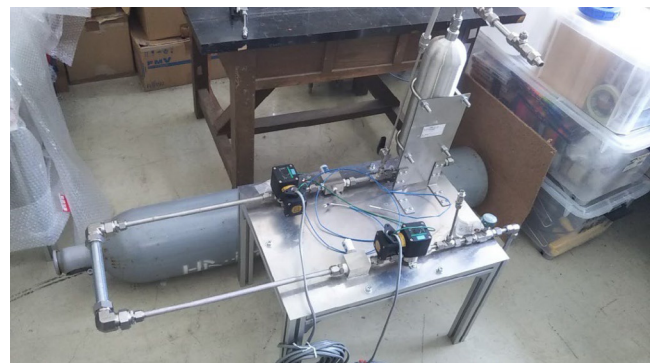


Figure 1 Experimental device for fluid hammer test.

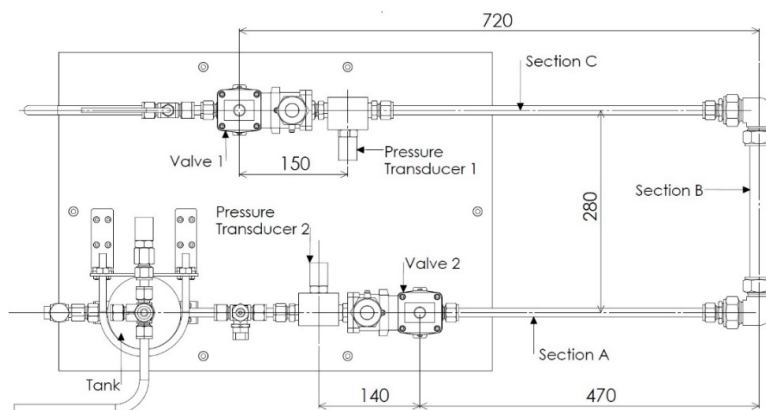


Figure 2 Layout of experimental device.

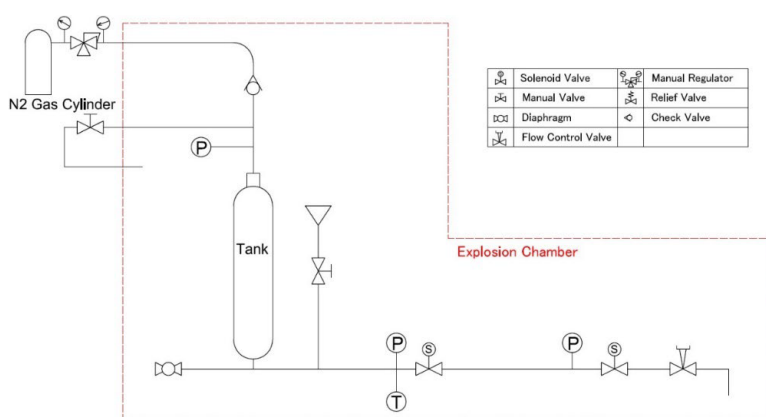


Figure 3 System diagram of experimental device.

pressure transducer, PGS-20KA by Kyowa Electronic Instruments[®], is also employed for the tank pressure measurement. The K-type thermocouple is installed near Pressure Transducer 2 for the liquid temperature measurement. The authors used the ultrasonic flowmeter FD-Q20C by Keyence[®] to measure the flow rate.

As shown in Figure 2, the nitromethane flowpath pipe is divided into three sections, Flow Section A, B, and C. Two 90-degree elbows are placed between those sections. This configuration was designed to make the test equipment as compact as possible while keeping the pipe length as long as possible to equip it into the explosion chamber. The inner and outer diameters of the Flow Section A and C are 10.7 mm and 12.7 mm, respectively. On the other hand, those are 23 mm and 25.4 mm for Flow Section B. The different pipe size is adapted for Flow Section B because it is adjusted to the size of the ultrasonic flowmeter.

The present device has a fluid-dynamically complicated flowpath configuration, such as different flow channel diameters or 90-degree elbows. Those complex configurations are due to the apparatus installation in the explosion chamber and the flowrate measurement. However, the actual propellant feed system may also have a complex propellant flowpath. The complexity of the nitromethane flowpath pipe system mimics such configuration.

2.3 Experimental methods

The present experimental device adapts the gas

pressurized feed system. Nitromethane is stored in the tank and pressurized by the nitrogen (N_2) gas to flow nitromethane through the flowpath pipe. The authors specified the four tank pressure conditions as 0.4, 0.6, 0.8, and 0.95 MPa. The tank pressure is limited to 1.0 MPaG in the present study due to the regulation of the High-Pressure Gas Safety Act in Japan. The tank pressure conditions in the present study are much lower than the impact pressure in the detonation tests by Bouyer et al.¹⁰⁾. The present study focuses on the propellant feeding system of a satellite RCS thruster. The tank pressure range is based on the feed pressure of the RCS thruster. For example, the MR-107V thruster by Aerojet Rocketdyne[®] has a feed pressure range from 0.55 MPaA to 2.6 MPaA¹⁶⁾. The present tank pressure range corresponds to a lower feed pressure range of the RCS thruster^{16),17)}. However, the tests in higher tank pressure conditions should be investigated in future studies.

Nitromethane flow test was conducted 3 times for each tank pressure condition. Prior to the nitromethane flow test, the authors conducted the fluid hammer tests of water to investigate the fluid-dynamical characteristics of the experimental device. The maximum flow rate in this device is $19.4 \text{ L} \cdot \text{min}^{-1}$ for water and $17.5 \text{ L} \cdot \text{min}^{-1}$ for nitromethane. The two pressure transducers are installed downstream of two valves to measure the static pressure in the nitromethane flow. The experimental data contain two static flow pressure, the tank pressure, liquid temperature, and the flowrate. Those experimental data are recorded in the data logger, DL850-M-HJ of Yokogawa Test and

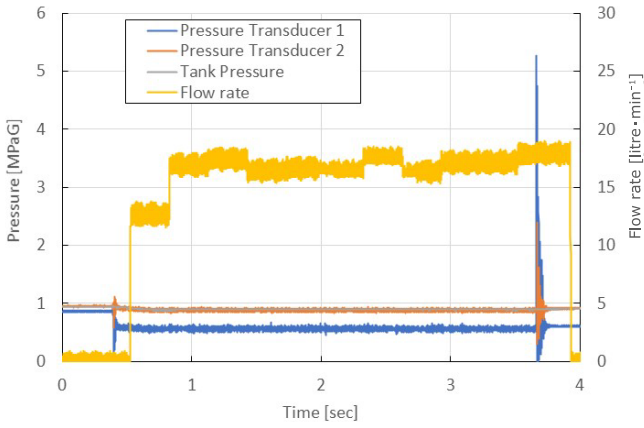


Figure 4 Time history data of fluid hammer phenomena test.

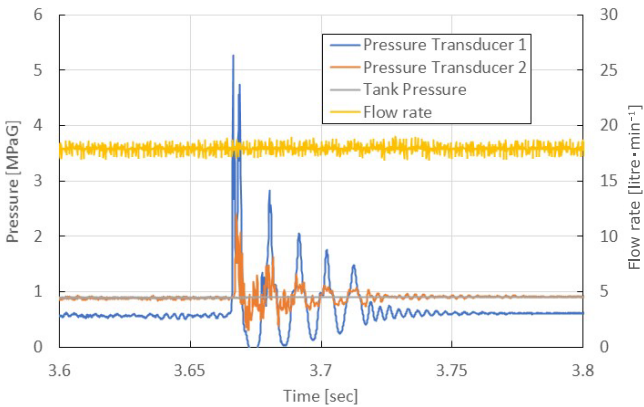


Figure 5 Detail of pressure rise in Figure 4.

Measurement Corporation®. The sampling rate of the data logger is 10 kHz during the test. The experimental procedure is described as follow.

- 1) Valve 1 and 2 are closed at first.
- 2) The liquid (water or nitromethane) is stored in the tank.
- 3) The tank is pressurized by the N_2 gas cylinder.
- 4) Valve 2 is opened, which is located upstream of Valve 1.
- 5) Valve 1 is opened and the liquid flows through the flowpath pipe.
- 6) After the flow rate becomes constant, Valve 1 and 2 are simultaneously closed.

3. Experimental results and discussion

3.1 Results of fluid hammer tests

Figure 4 shows the typical time histories data in the fluid hammer tests, which indicates the rapid pressure rise of the fluid hammer effect. Figure 5 shows the details of the pressure rise in Figure 4. The time history data of the Pressure Transducer 1 in Figure 5 indicates the damped vibration. Moreover, the pressure rise of Pressure Transducer 1 is higher than pressure transducer 2. The Pressure Transducer 1 is installed 150 mm upstream of Valve 1. This location is within the confinement section. Thus, the rapid pressure rise of Pressure Transducer 1 is more prominent than that of Pressure Transducer 2. The authors conducted the fluid hammer tests in the four tank pressure conditions

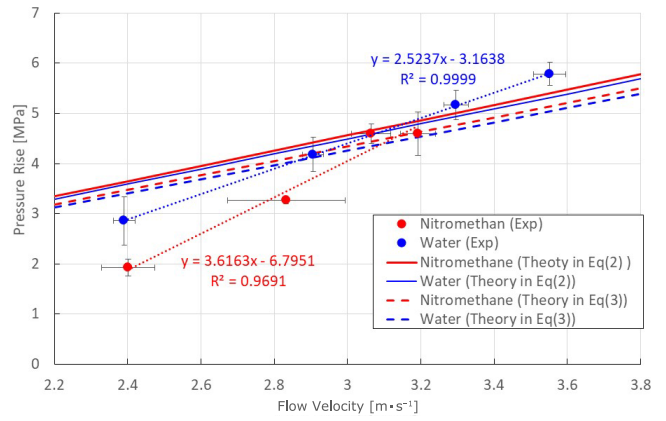


Figure 6 Correlation between flow velocity and fluid hammer pressure rise.

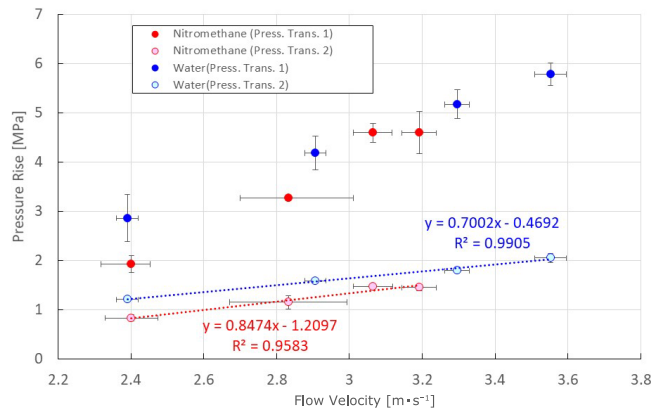


Figure 7 Fluid hammer pressure rises at Pressure Transducer 1 and 2.

to verify the explosion risk of nitromethane. As a result, no explosion occurred for nitromethane in any case of the present study.

Figure 6 shows the correlation between the average flow velocity and the pressure rise of fluid hammer effect at Pressure Transducer 1 for water and nitromethane. The pressure rise of the fluid hammer effect is defined as the difference of the maximum peak pressure to the average static pressure before the valves are closed. The average flow velocity is defined to divide the volumetric flow rate by the cross-section area of the flowpath tube. The fluid hammer tests are done three times for each tank pressure condition. The data in Figure 6 is the average of three tests, and those error bars indicate the standard deviation. The average pressure rise in the tank pressure condition of 0.95 MPaG is 4.59 MPa, and the maximum pressure rise is 4.95 MPa in this tank pressure condition. This value is the maximum pressure rise in the present study, which does not occur explosion. Further investigation is necessary to determine the actual limit not to occur explosion for nitromethane.

The theoretical pressure rises in Equations (2) and (3) are also shown in Figure 6. With the consideration of the elasticity of the pipe material, the pressure propagation velocity in Equation (3) is a little less than that in Equation (2). Thus, the pressure rise by Equation (3) is also lower than Equation (2). The present data indicate that the

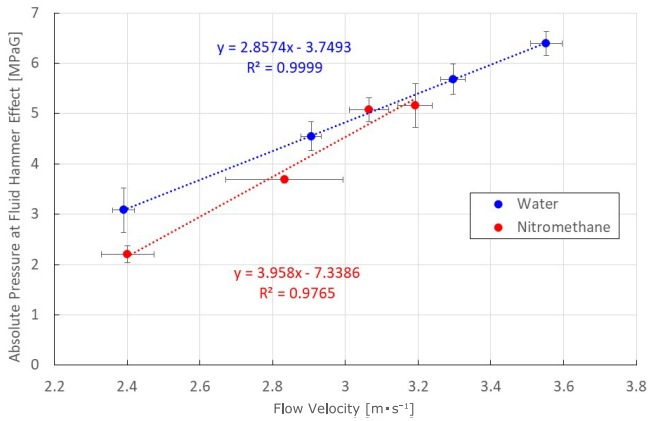


Figure 8 Maximum absolute pressure for fluid hammer phenomena.

pressure rise by the fluid hammer effect is linearly proportional to the flow velocity. The experimental pressure rises are close to the theoretical values if the flow velocity is more than $3.0 \text{ m} \cdot \text{s}^{-1}$. However, the experimental pressure rise tends to be lower than the theoretical prediction in lower flow velocity conditions. In addition, the experimental pressure rises of water exceed the theoretical values for flow velocity more than $3.0 \text{ m} \cdot \text{s}^{-1}$. The experimental pressure rises of nitromethane are equal to or less than water. The average pressure rise by fluid hammer effect is 4.59 MPa in the tank pressure condition of 0.95 MPaG . The maximum pressure rise is 4.95 MPa , and the maximum flow velocity is $3.24 \text{ m} \cdot \text{s}^{-1}$. Unfortunately, the present study did not do the test of the flow velocity higher than $3.24 \text{ m} \cdot \text{s}^{-1}$.

Figure 7 shows the fluid hammer pressure rises at Pressure Transducer 2 compared with Pressure Transducer 1. The fluid hammer pressure rises at Pressure Transducer 2 are dramatically less than Pressure Transducer 1. A surge tank is often used to mitigate the fluid hammer effects. The surge tank is the storage reservoir containing gas and liquid, which connects to the flowpath. The flow section of Pressure Transducer 2 connects to the nitromethane tank directly. N_2 gas cylinder feeds Nitrogen gas to this tank during the test. Thus, the nitromethane tank functions as a surge tank when two valves shut off. That results in the lower pressure rise at Pressure Transducer 2. In addition, the correlation between flow velocity and pressure rise of nitromethane is very similar to water for Pressure Transducer 2. The product of density and sonic speed in nitromethane is about the same as that in water. This fact corroborates the pressure rise behaviors of nitromethane and water in Figures 6 and 7.

Figure 8 shows the absolute peak pressure by the fluid hammer effect. Those error bars indicate the standard deviation. The results in Figure 8 show the linear proportion between the absolute peak pressure and the flow velocity. The average absolute peak pressure of nitromethane is 5.15 MPaG in the tank pressure condition of 0.95 MPaG , and the maximum one is 5.52 MPaG . Moreover, the absolute peak pressure of nitromethane is the same as or less than water. The results in Figures 6 and 8 certified that the peak pressure of the fluid hammer phenomena less than 5.15

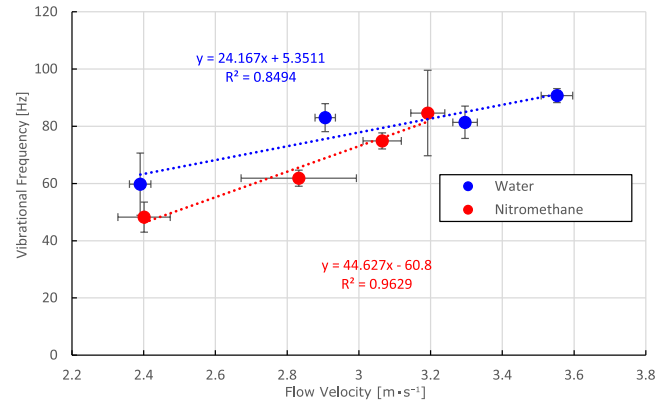


Figure 9 Pressure oscillation frequency in fluid hammer test.

MPaG does not occur explosion. However, the present investigation does not imply that the value of 5.15 MPaG is equal to the upper limit not to occur explosion. The determination of the actual limit occurring explosion of nitromethane requires further investigation.

The pressure oscillation of the fluid hammer shows the damping behavior, as indicated in Figure 4. The authors calculated the pressure oscillation frequency by using Discrete Fourier Transformation. Figure 9 shows the pressure oscillation frequency as a function of the flow velocity. In the present experimental device, the flow path between Valve 1 and 2 become the confinement section after those valves shut off. The total length of the confinement section is 1.47 m , as shown in Figure 2. The fluid hammer pressure wave propagates back and forth between the confinement sections. The pressure oscillation in Figure 4 represents the fluid hammer pressure wave propagation. The maximum oscillation frequency is close to 100 Hz in the fluid hammer phenomena of nitromethane. The pressure propagation velocity is determined as $265 \text{ m} \cdot \text{s}^{-1}$ from this frequency. This propagation velocity is only one-fifth of the sonic speed of nitromethane. However, the maximum pressure rise of the fluid hammer phenomena is close to the theoretical prediction in which the pressure propagation speed is equal to its speed of sound. The present experimental device has a complicated flow path configuration, such as different inner diameters or 90-degree elbows. The pressure wave propagates with a speed of sound in the straight flowpath and may delay at 90-degree elbows. Therefore, the assumption that the pressure wave propagates with the speed of sound is reasonable.

3.2 Design criteria of Nitromethane propellant feed system

The present experimental data can provide the design criteria of the nitromethane propellant feed system. As shown in Figures 6 and 8, the average pressure rise and the absolute pressure in the tank pressure condition of 0.95 MPaG are 4.59 MPa and 5.15 MPaG , respectively. The average flow velocity is $3.19 \text{ m} \cdot \text{s}^{-1}$ in this condition. Thus, the authors recommend that the peak pressure of the fluid hammer phenomena should be less than 5.15 MPaG in the design of the nitromethane feed system. Equation (1) can estimate the fluid hammer pressure rise. This estimation

considers the pressure propagation velocity as the sonic speed of the fluid. Equation (3) has been widely used to predict the pressure propagation speed in the fluid hammer phenomena. Allievi's equation considers the elasticity of pipe material and evaluates the pressure propagation velocity lower than the speed of sound. Therefore, the speed of sound in Equation (2) is more desirable than Allievi's equation in Equation (3) to evaluate the pressure propagation velocity because of the safety margin.

However, the theoretical estimation of the fluid hammer pressure rise may contain errors. Thus, its experimental evaluation is required. The present experimental data indicate that the fluid hammer phenomena of nitromethane have similar fluid dynamic behaviors to those of water. Thus, the authors recommend conducting the fluid hammer test by using water to verify the safety of the nitromethane propellant feed system if the flow velocity is less than $3.2 \text{ m} \cdot \text{s}^{-1}$. In the present fluid hammer tests, the pressure rise and the absolute peak pressure of water are higher than nitromethane. Therefore, using water to estimate the fluid hammer pressure rise of nitromethane is desirable from the viewpoint of the safety margin.

4. Conclusion

The present study conducted the fluid hammer tests of nitromethane and evaluated its explosion risk. The tank pressure conditions are 0.4, 0.6, 0.8 and 0.95 MPaG. The summary of the conclusion in the present study is listed below.

1. No explosion occurred in any condition of the present study. In the tank pressure condition of 0.95 MPaG, the maximum peak pressure is 5.52 MPaG in the nitromethane fluid hammer test. The average peak pressure of the fluid hammer effect is 5.15 MPaG, and the flow velocity is $3.19 \text{ m} \cdot \text{s}^{-1}$. The present investigation confirms that explosion does not occur at this pressure level. However, the peak pressure of 5.15 MPaG is not the upper limit not to occur explosion.
2. The correlation between pressure rise and the flow velocity in fluid hammer phenomena for nitromethane is close to the theoretical prediction of the Joukowsky equation in the flow velocity condition of more than $3.0 \text{ m} \cdot \text{s}^{-1}$. The experimental fluid hammer pressure rise of nitromethane tends to be lower than the theoretical prediction if the flow velocity is lower than $3.0 \text{ m} \cdot \text{s}^{-1}$. Therefore, the Joukowsky equation is useful for predicting the pressure rise of the fluid hammer effect in the design of the nitromethane propellant feed system.
3. The behaviors of nitromethane in the fluid hammer, such as peak pressure and oscillation frequency, are similar to water. The absolute peak pressure of nitromethane is a little lower than water. Thus, it is recommended to use water for the fluid hammer test of the nitromethane feed system because of its safety.
4. The tank pressure range corresponds to a lower feed pressure range of the RCS thruster in the present study. The present experimental results indicate the safety of nitromethane propellant for the satellite RCS thruster in its low feed pressure condition. However, the further

investigation in higher feed pressure conditions is necessary in future studies.

Acknowledgement

The authors would like to represent our appreciation to Mr. Ryo Kanbara and Mr. Hikaru Sasaki, undergraduate students at the Department of Mechanical and Aerospace Engineering, Muroran Institute of Technology, for their contribution to this study. The authors would like to thank Apollo Fukuchi, the associate professor at Saitama Institute of Technology, for advice on a reaction control system of a satellite. This study was supported by Institute of Industrial Nanomaterials, the University of Kumamoto, and f^3 Engineering Education and Research Center, Faculty of Engineering, the University of Hokkaido.

Reference

- 1) T. Nelson, J. Bjorgaard, M. Greenfield, C. Bolme, K. Brown, S. McGrane, R. J. Scharff, and S. Tretiak, *J. Phys. Chem. A*, **120**, 519–526 (2016).
- 2) S. Tanaka, I. Bataev, D. Inao, and K. Hokamoto, *Appl. Energ. Combust. Sci.*, 1–4, 100005 (2020).
- 3) Y. Takahashi, S. Kubota, T. Saburi, Y. Ogata, H. Yamachi, J. Nakamori, and K. Uenishi, *Sci. Technol. Energ. Mater.*, **82**, 161–169 (2021).
- 4) J. D. Clark, "Ignition! : An Informal History of Liquid Rockets Propellants" Rutgers University Press, NJ (1972).
- 5) J. Benziger, "A Mechanistic Study of Nitromethane Decomposition on Ni Catalyst" Air Force Office of Scientific Research TR-83-0405 (1982).
- 6) E. Boyer and K. K. Kuo, AIAA Paper, 2006-361 (2006).
- 7) D. Fukuda, K. Moriya, K. Kaneko, K. Sasaki, R. Sakamoto, and K. Hidani, *Int. J. Fract.*, **180**, 163–175, 10.1007/s10704-013-9809-4 (2013).
- 8) K. Uenishi, H. Yamachi, K. Yamagami, and R. Sakamoto, *Constr. Build Mater.*, **67B**, 170–179, 10.1016/j.conbuildmat.2014.05.014 (2014).
- 9) S. Tanaka, M. Nishi, M. Yamaguchi, I. Bataev, and K. Hokamoto, *J. Dyn. Behav. Mater.*, **6**, 53–63, 10.1007/s40870-019-00227-6 (2020).
- 10) V. Bouyer, I. Darbord, P. Herve, G. Baudin, C. L. Gallic, F. Clement, and G. Chavent, *Combust. Flame*, **144**, 139–150 (2006).
- 11) "Accident near Mt. Pulaski, ILL", Interstate Commerce Commission Ex. Parte No.213 (1958).
- 12) ATAMAN Chemicals, "Nitromethane (Nitromethan)", <https://atamankimya.com/sayfalar.asp?LanguageID=2&cid=3&id=11&id2=3836>, (accessed: 17-April-2022). (Online).
- 13) ANGUS Technical Data Sheet, ANGUS Chemical Company (1998).
- 14) M. Greenspan and C. E. Tschiegg, *J. Res. Natl. Bur. Stand.*, **59**, 249–254 (1957).
- 15) A. Cwiklinska and C. M. Kinart, *J. Chem. Thermodyn.*, **43**, 420–429 (2011).
- 16) Aerojet Rocketdyne, "In-Space Propulsion Data Sheet", <https://www.rocket.com/sites/default/files/documents/In-Space%20Data%20Sheets%204.8.20.pdf>, (accessed: 13-April-2022). (Online).
- 17) G. Fujii, D. Goto, H. Kagawa, S. Murayama, K. Kajiwarra, H. Ikeda, N. Shinozaki, T. Nagao, N. Morita, and E. Yabuhara, *Trans. J. Space Technol. Sci.*, **28**, 37–47 (2013).